Architecture
Image Studies

Vol.7, Issue 1, pp.692-712, 2026
DOI: https://doi.org/10.62754/ais.v7i1.897

https://journals.ap2.pt/index.php/ais/index

Spatial Analysis of Flood Risk in Manavgat

Osman Nasanlı[1], Devrim Türkan Kejanlı[2], Nurullah Tan[3]

Abstract

The number of natural disasters is increasing day by day due to climate change and pop-ulation growth. Disasters increase loss of life and property when city plans are prepared without sufficient consideration and land use decisions are made. In 2010, 2014 and 2021, floods in Antalya caused significant material losses in many districts. In recent years, in-creasing floods in the city centre of Manavgat, Antalya, have caused economic losses and expanded their area of impact. In this context, the aim of this study is to analyse the rela-tionship between land use and floods in Manavgat using the Analytical Hierarchy Pro-cess (AHP) and Geographic Information System (GIS) techniques, thereby offering rec-ommendations for risk reduction. The study covers the identification of areas at risk of flooding and the development of settlement proposals for these areas. An analysis map has been prepared within this scope. Risk increases in low-altitude agricultural areas and urban areas with high rainfall, while it decreases in areas with low rainfall, high altitude and forested areas. Therefore, land use should be planned according to scientific and geo-graphical data, construction should be restricted in hazardous areas, permeable surfaces should be increased, and the destruction of forested areas should be prevented.

Keywords: *Urban land use; Flood risk; GIS; AHP*

Introduction

Due to climate change and rapid urbanisation, floods are among the most destructive disasters worldwide, causing both economic losses and loss of life [1,2,3,4]. The report by the Intergovernmental Panel on Climate Change (IPCC) states that extreme weather events and floods will become more frequent and severe in the future [5]. Particularly in areas with high levels of urbanisation, rainwater runoff onto impermeable surfaces increases the risk of flooding. According to recent research, while 1.81 billion people were living under a 100-year flood risk in 2020, this number is projected to reach 1.93 billion by 2100. It is stated that 21.1% of this increase is due to climate change, 76.8% to population growth and urbanisation, and 2.1% to the combined effect of these three [6]. It is a well-known fact that areas at risk of flooding and inundation will increase due to climate change and population growth. According to a 30-year observational study, floods have increased by approximately 26.6 per cent worldwide. This rate is 44.4 per cent for the European continent and 26.4 per cent for the American continent [7]. Between 1975 and 2021, 901 people lost their lives due to floods and flash floods in Turkey. According to current data, floods cause an economic loss of 300 million TL every year [8]. It is reported that floods and torrential rains caused 35 per cent of the damage among the meteorological disasters experienced in Turkey in 2024 [9]. The most important reason for this is that, while climate change and urbanisation are increasing, geological and climatic data are not being taken into account in land use [10].

Unplanned urbanisation and the development of high-risk areas exacerbate the effects of natural disasters, leading to significant loss of life and property. This situation has become even more pronounced due to the effects of climate change; sudden and heavy rainfall, heatwaves and droughts have significantly increased the risk of disasters in cities [11]. Antalya, located in the Mediterranean Region, experiences an average of 15 heavy downpours per year [12]. The flood and torrential rain events between 1975 and 2020 were examined and analysed by AFAD (Disaster and Emergency Management Presidency) using data from the State Hydraulic Works 13th Regional Directorate and the Meteorology 4th Regional Directorate [13]. According to the analyses conducted, flood risk is highest in the districts of Konyaaltı, Muratpaşa, Kepez, Aksu, Döşemealtı, Kumluca, Finike, Kemer, Manavgat,

[1] osmannasanli@artuklu.edu.tr. ORCID: https://orcid.org/0000-0003-1706-3086 (corresponding author).
[2] turkanak@dicle.edu.tr. ORCID: https://orcid.org/0000-0002-0476-2307
[3] nurullah49@gmail.com. ORCID: https://orcid.org/0000-0003-1316-4592

Demre and AlanyaIt has been determined that the risk is lower in the districts of İbradı, Akseki and Gündoğmuş, which are located at higher altitudes [13]. In particular, the frequency and impact of flooding events in the Manavgat district have increased in recent years. Frequent flooding in the city centre is causing damage to numerous homes, businesses and infrastructure. The floods that occurred on 16 December 2010 and 25 October 2014 caused significant material damage, while the heavy rainfall on 10 October 2021 affected residential areas and agricultural lands along the Manavgat River [13]. Finally, it has been reported that numerous homes and businesses in the city centre of Manavgat were damaged in the flood that occurred on 21 December 2024 [14].

Today, due to the increasing population in Manavgat, construction and flood risk are on the rise. In this context, it is important to identify flood-prone areas and develop settlement proposals. This study examines the development stages of urbanisation practices in Manavgat and assesses land use in terms of flood risk. Settlement decisions made by taking into account the city's current data, primarily scientific, climatic and geographical data, significantly reduce the risk of disasters. The main objective of this study is to analyse the relationship between land use and floods in Manavgat using the Analytic Hierarchy Process (AHP) method and Geographic Information System (GIS) techniques, and to offer recommendations for reducing flood risks.

The combined use of CBS and AHP methods offers a robust approach to disaster risk assessments from both a spatial and analytical perspective. CBS enables the analysis of the geographical distribution of risk factors and the visualisation of results, while the AHP method allows for the determination of the importance level of multiple criteria. The integration of these two methods systematises the decision-making process in the risk analysis of natural disasters [15,16]. Indeed, the AHP method was used to assess resilience to flood risk in the city of Tehran [17]. Similarly, a flood risk map was created in the Pune region of India using the CBS and AHP methods; flood risk was determined based on seven criteria, including rainfall, slope and soil [18]. In China's Hunan province, a CBS-based index was developed to assess flood risk through spatial risk maps [19]. Looking at examples from Turkey, sensitivity analyses have been carried out in the Ladik Lake Basin using AHP and CBS to assess vulnerability to disasters such as floods and earthquakes [20]. The causes of the flood disaster that occurred in Şanlıurfa in 2023 were analysed with the help of CBS; it was evaluated based on criteria such as slope and geology [21]. In the city of Antakya, floods, erosion and ground movements were analysed using CBS, and recommendations were made for a disaster management model [22]. When examining previous studies conducted specifically on the city of Manavgat, it is seen that CBS-based maps were created at the neighbourhood level in order to determine the priority intervention areas where water-sensitive urban design could be implemented [23]. However, no study has been found in the literature where risk analysis maps produced using CBS and AHP together have been evaluated in conjunction with urbanisation practices. It is believed that this study, prepared using this methodological integration, will make an original contribution to the literature.

Materials and Methods

Manavgat district is located within the boundaries of Antalya province in the Mediterranean Region at 36° 47' 12'' north latitude and 31° 26' 49'' east longitude [24]. Manavgat, located in the east of Antalya province, is bordered to the north by the districts of Derebucak in Konya and Sütçüler in Isparta; to the east by the districts of İbradı, Akseki, Gündoğmuş and Alanya, which belong to Antalya province; to the west by the district of Serik in Antalya; and to the south entirely by the Mediterranean coastline, stretching for 64 kilometres (Figure 1), [25].

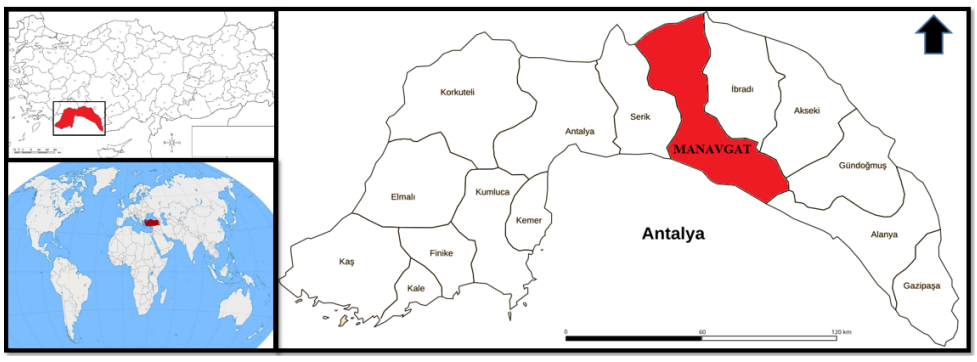

Figure 1. Manavgat district location map

The city centre is located on relatively flat land approximately 4-5 kilometres inland from the coast. The city's morphological structure consists of a wide plain with fertile agricultural land, the Taurus Mountains rising to the north, and the Mediterranean Sea to the south. Approximately 74% of the district's land is mountainous, 11% is flat, and 15% is hilly. When examining the Manavgat settlement, it can be seen that it developed on gentle slopes with gradients between 0-5% and 5-15%. In the south-west, north, east and some western parts of the settlement, there are areas where the gradient exceeds 20% in places. The steepest area in the town is the wooded area in the centre of the settlement, where there are steep slopes with gradients exceeding 30% [9]. The Alara River separates the district of Alanya from the district of Serik via the Köprüçay Valley [26]. With the gradual increase in elevation towards the north, local variations in climate characteristics are observed [27,28].

In the area between the coast and the foothills, numerous plains of varying sizes have formed due to the accumulation of alluvial material carried by rivers [29]. The geography of Manavgat consists of alluvial, conglomerate and fill areas stretching from the sea to the Taurus Mountains in the north [30]. Running east-west parallel to the Mediterranean Sea, the Taurus Mountains have enabled Manavgat to develop northwards; the city has expanded in the east, west, south and north directions (Figure 2).

Figure 2. Manavgat city centre in 2025

Manavgat has a typical Mediterranean climate, with hot, dry summers and mild, rainy winters [29]. The average annual rainfall in the district is 1043 mm, with an average of 76 rainy days per year; the highest rainfall occurs in December, while the lowest rainfall occurs in July and August (Figure 3), [26]. According to data from the General Directorate of Meteorology, rainfall is expected to increase by approximately 5 per cent by 2040 [31,23].

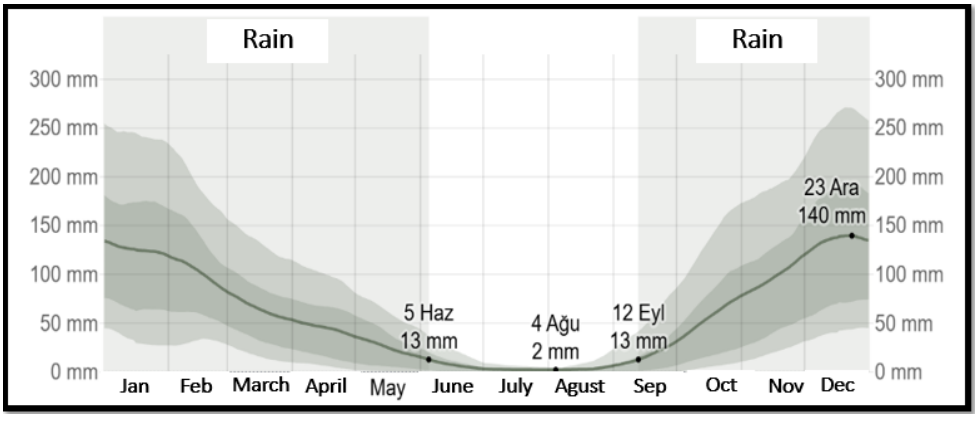

Figure 3. Monthly average rainfall in the Manavgat region [32].

Originating in the Western Taurus Mountains, the Manavgat River (Figure 4), which is 93 km long and has a drainage area of 1,675 km², is one of Turkey's most regular and high-flow rivers, reaching the Mediterranean Sea from the Manavgat Plain [23].

Figure 4. Manavgat River

The city centre formed around the Manavgat River has been affected many times by floods triggered by excessive rainfall and various natural events, causing significant material damage to the city. The direction and speed of the winds, and whether they originate from land or sea, can create different effects [33], The lodos, a particularly warm and dry southwesterly wind, raises air temperatures on the days it blows and, when blowing strongly, can cause high waves along the Mediterranean coast, leading to flooding [34]. One such area where this phenomenon has been observed is Manavgat, where strong southerly winds typically bring rainfall. The waves formed where the Manavgat River meets the sea directly impact the coastline and settlements. Furthermore, the southerly wind's flow towards the sea hinders the river's course, increasing flooding and causing the Manavgat River to overflow. Indeed, on 12 January 2022, as a result of the severe south-westerly wind that affected Manavgat, waves crashed onto the shore, leaving numerous businesses under water [35]. The flood risk map prepared by the State Hydraulic Works also shows that flood risk is higher in areas close to the coast (Map 1).

Map 1. Manavgat River flood risk map [36].

Historical sources indicate that approximately 500 years ago, in the region southeast of Manavgat, now known as the Ulualan Plain, there was a large lake area (Figure 5) surrounded by drainage channels, referred to as "Lake Manavgat" [30,23].

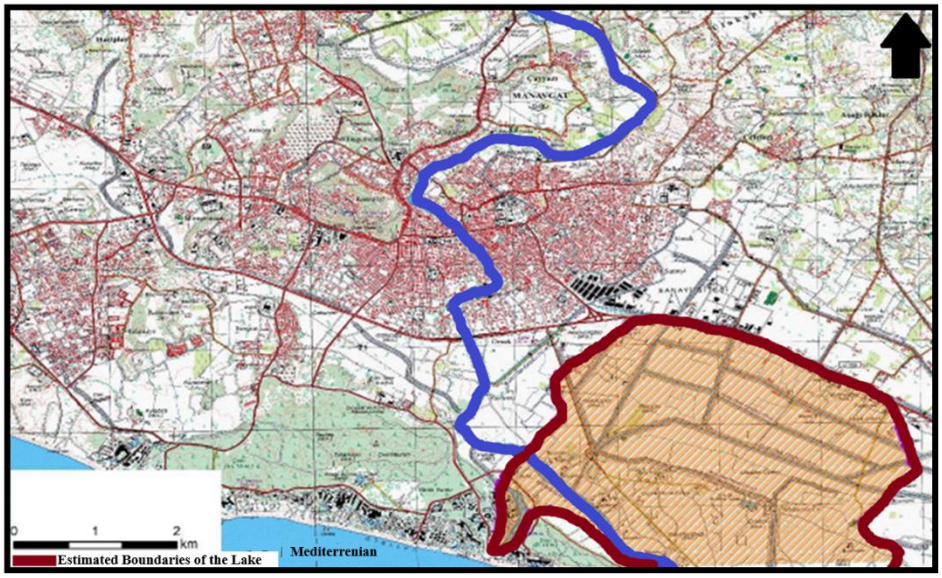

Figure 5. Estimated boundaries of Yalı Lake, located in the southeast of Manavgat [25].

Today, the numerous drainage channels and advanced drainage network in the Ulualan Plain confirm that this area was once a lake bed. As in the past, it continues to exist as the most important natural feature hindering the city's horizontal expansion towards the southeast [25]. Another natural structure located in the centre of Manavgat, Türk Beleni (Figure 6), is situated at a higher elevation than its surroundings and is surrounded by steep slopes [30].

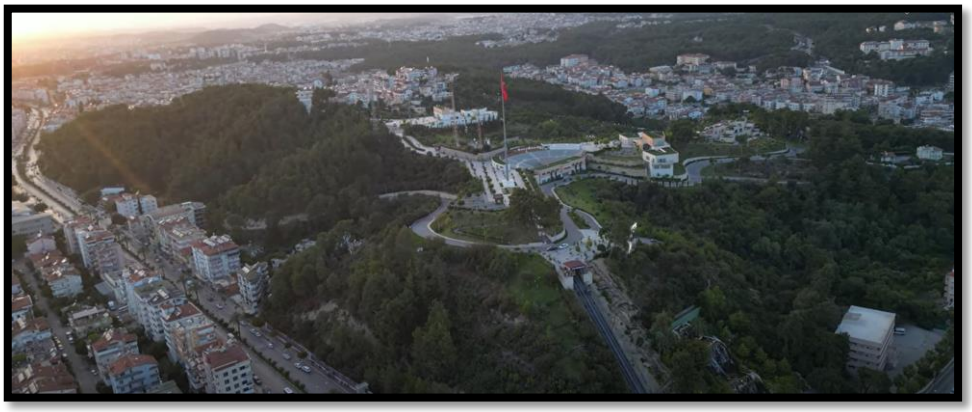

Figure 6. Turkish Beleni

The history of settlement in Manavgat and its surroundings dates back to ancient times, particularly the Hellenistic and Roman periods. One of the oldest settlements in the region, Side was established on the historic peninsula southwest of Manavgat and, thanks to the advantages afforded by its geographical location, became an important trade and port city in the ancient world [37]. Side, which emerged as a major trading centre during the Roman Empire, particularly in the 1st and 2nd centuries, lost its importance by the 9th century due to various political and economic reasons. It was completely abandoned during the Middle Ages as Antalya gained supremacy in Mediterranean trade. In the 13th century, the Turks who came to the region laid the foundations of what is now the city of Manavgat, approximately 6-7 km northeast of Side, on the west bank of the Manavgat River, choosing the area around Hisar (Zindan) Castle as their settlement [25]. In the first half of the 16th century, Manavgat was located at the foot of Hisar Castle, 4-5 kilometres inland from the sea (Figure 7). There were no settlements on the eastern side during those years [30].

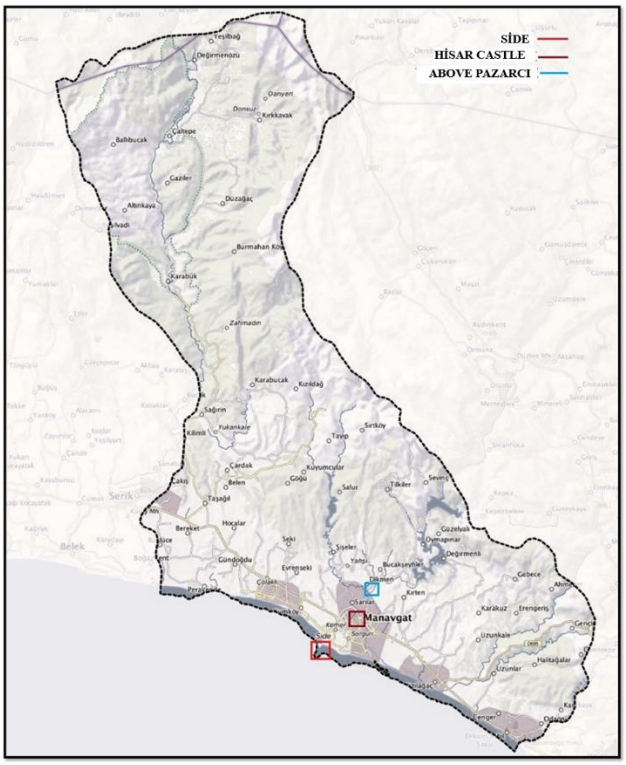

Figure 7. The first settlement areas in Manavgat and Side

In 1455, the city's population was recorded as 400-600, in 1575 as 225, and in 1872 as 3,232. At the beginning of the 20th century, the city resembled a small neighbourhood (Figure 8), [38,39,40].

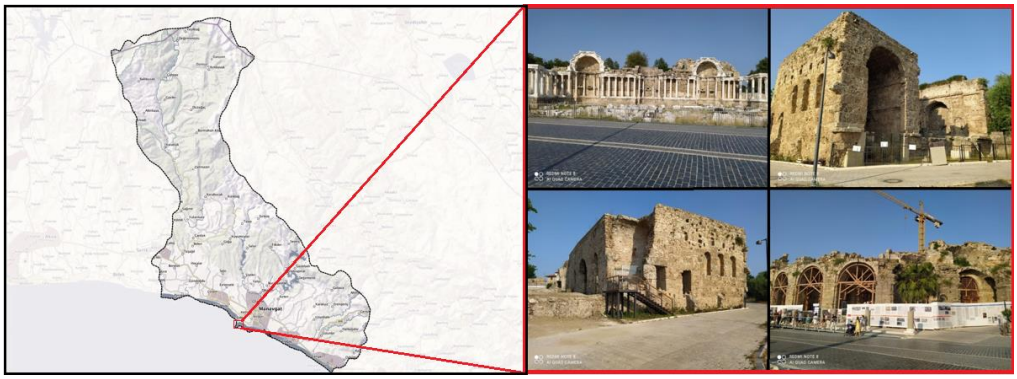

Figure 8. Side settlement

The permanent settlement and horizontal development of the city began in the early 20th century; the area consisting of a few buildings in the Hisar neighbourhood on the west bank of the Manavgat River and around the present-day Manavgat Bridge (Figure 9) formed the core of the settlement [30,41].

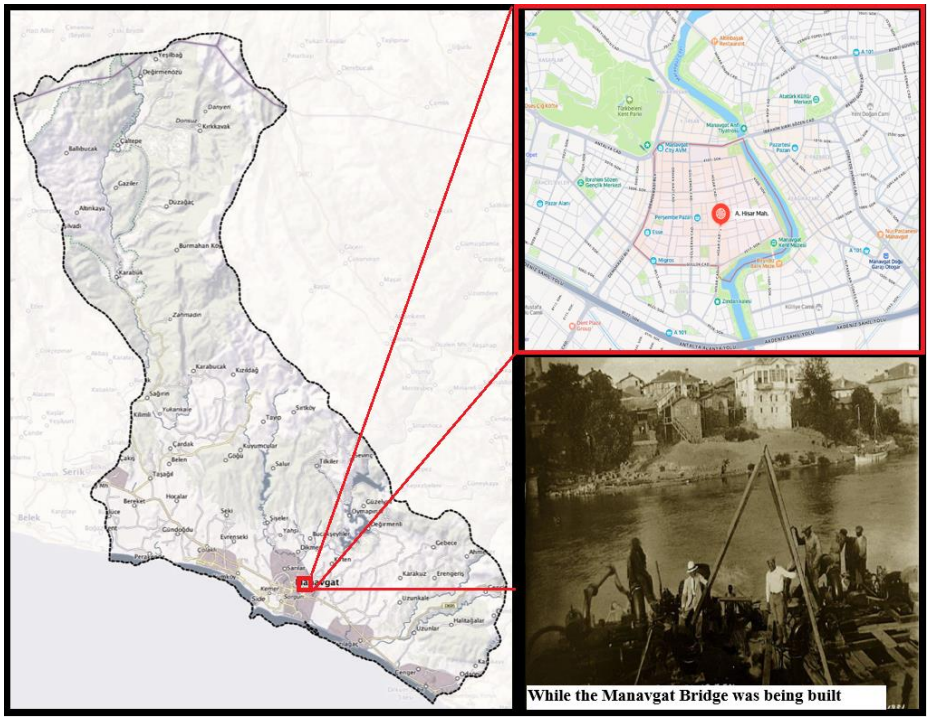

Figure 9. Hisar Neighbourhood and Manavgat Bridge under construction [25].

From the 1900s onwards, the city developed rapidly horizontally through the draining of marshes, bridge and infrastructure investments, migration, tourism and industrial investments. Today, it has spread across a wide geographical area, with settlements concentrated on the east and west banks of the Manavgat River [25]. In 1913, with the establishment of the district organisation, the name "Manavgat" gained official status. During the Republican era, rapid development began, particularly on the eastern and western banks of the river [30]. In 1927, Manavgat had an administrative area of 2,140 km² and a population of 655. In the 1930s, the construction of the Manavgat Bridge physically connected the eastern and western banks. Urbanisation has been concentrated on the eastern side in recent years, leaving the western side largely undeveloped [39]. Administrative changes led to Manavgat expanding to 2,749 km² in 1945 and 2,283 km² between 1950 and 1960. Migration also increased due to the draining of marshes and economic developments. From the 1950s onwards, Above Pazarcı Neighbourhood (Figure 10) on the eastern side of Manavgat was chosen due to its low risk of flooding and malaria, and expansion towards the west began [25,42]. During these years, the city expanded towards Above Pazarcı and westwards, and the urban area grew rapidly with tourism and industrial investments [43,44].

Figure 10. View of Yukarı Pazarcı Mahallesi in 1945 [25].

In the 1950s, the Yukarı Pazarcı neighbourhood, particularly on the eastern bank of the Manavgat River, was less affected by floods and inundations due to an elevation difference of approximately 25-30 metres and conglomerate soil; alluvial areas were used for agricultural activities [25]. Until 1953, the eastern side of the Bridge had a more dense settlement than the western side [39].

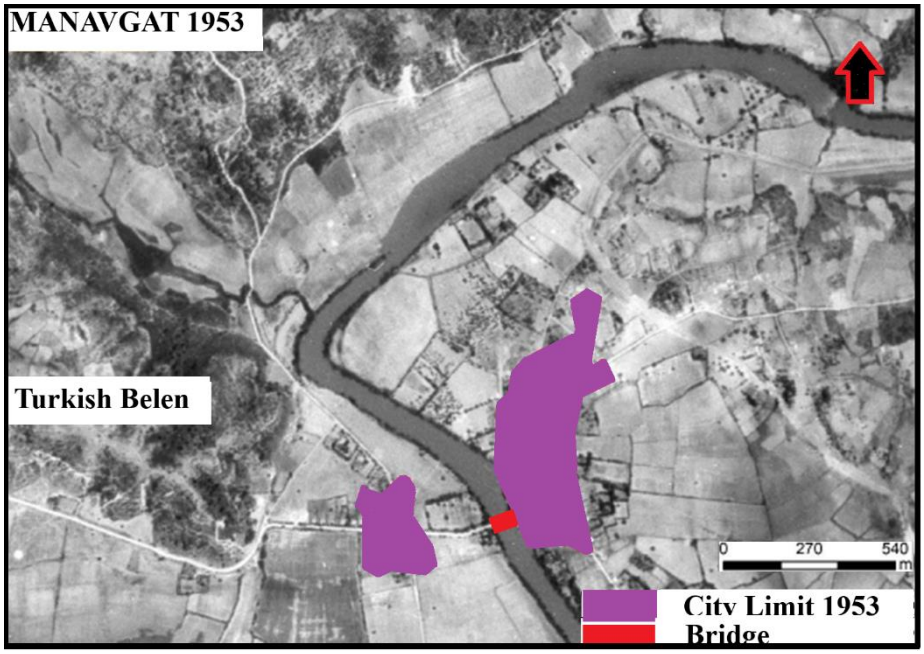

Figure 11. Aerial photograph of Manavgat in 1953 [25].

The first town plan for Manavgat was drawn up in 1957 [25]. In the 1960s, population growth accelerated construction; Antalya Street became a commercial hub (Figure 12), and public buildings were constructed on the west bank of the river. Due to the growing population, cotton fields have been expropriated and converted into schools and sports grounds [40].

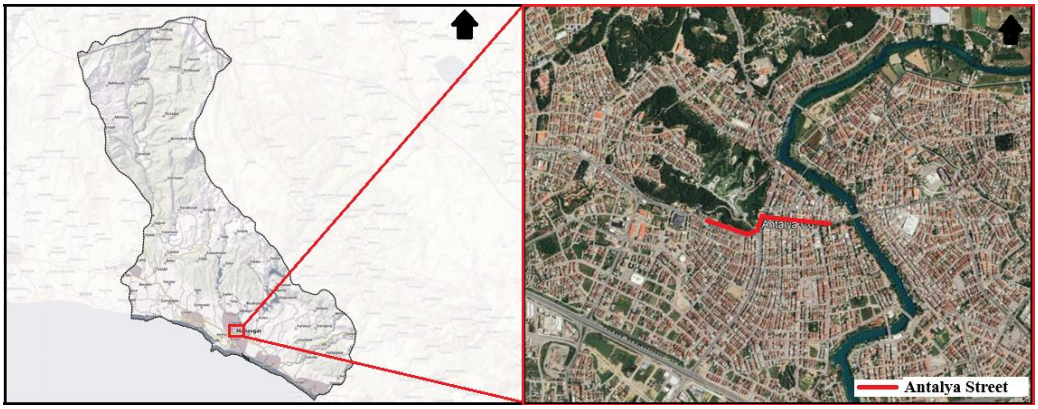

Figure 12. Antalya Street and its surroundings

From the first development plan until 1971, the urban area increased by 58.9 per cent, with the formation of settlement areas from arable land concentrated particularly in the district centre, while forest areas decreased by 0.8 per cent and the plan was revised in 1975 [27]. From 1975 to 1983, the city expanded northwards into alluvial areas (Figure 13). Due to tourism and migration, the urban area has increased from 86.3 hectares to 372.7 hectares, with the settlement in the historic region of Side reaching 61.4 hectares [30].

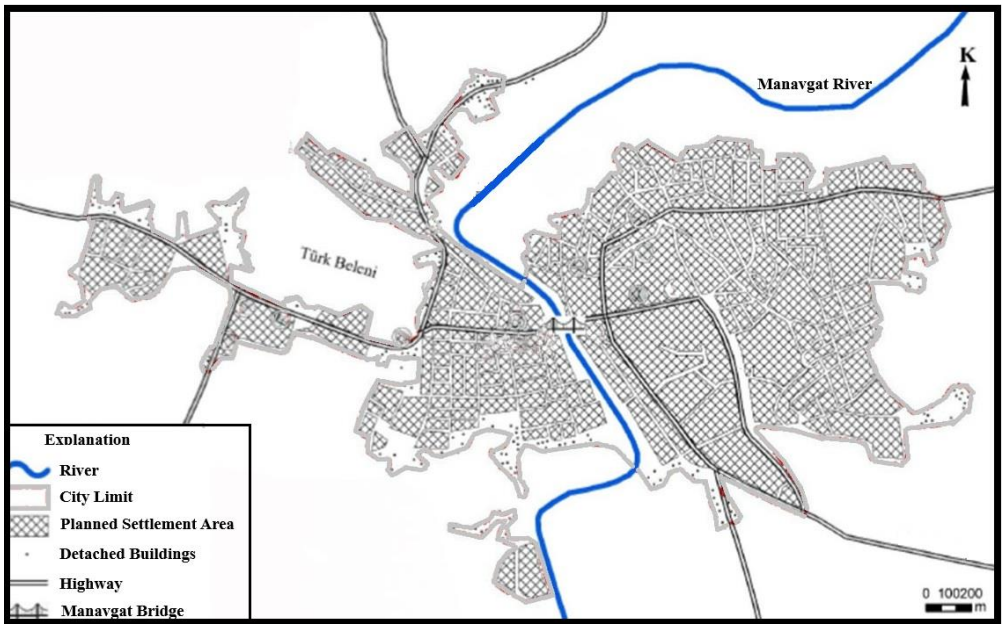

Figure 13. Manavgat city centre 1983 settlement area [25].

Until 1986, growth was observed in the city's industrial, tourism, commercial and transport sectors; forested areas decreased while arable land increased (Yıldırım, 2013). During these years, the Oymapınar and Manavgat Dams, drainage and canal works were aimed at controlling floods. In these years when shanty towns have increased, horizontal development has accelerated in the east and west [45]. With the 1984 and 1990 development plans, new streets and avenues were opened, new residential areas were designated due to the impact of tourism, and agricultural lands, forests and dunes were opened up for settlement [27,40]. The city's population rose to 38,498, with the annual population growth rate reaching its highest level to date at 11.6 per cent [46]. In the 1990s, development accelerated in the north with the opening of the Alanya-Antalya motorway [25]. In 1995, the Manavgat settlement north of the D-400 motorway reached 489.8 hectares, while Side reached 720.2 hectares; the western coastline of Side was declared a tourism zone. Until 2012, planning decisions accelerated the development of Side towards the north and Manavgat towards the south. By 2017, the city had expanded in all directions (Figure 14) and reached 3,851.6 hectares [30].

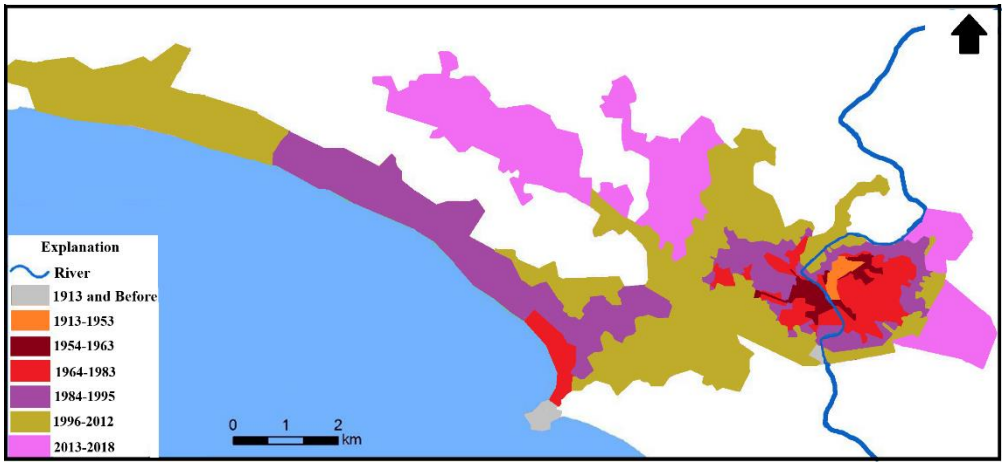

Figure 14. Map of the horizontal development of Manavgat city [30].

From the 1950s to 2025, wooded areas have decreased and agricultural and urban areas have increased almost every year (Figure 15). The main reasons for these transformations are population growth, the expansion of agricultural activities, the application of modern agricultural techniques, and the construction of the Manavgat and Oymapınar dams [27].

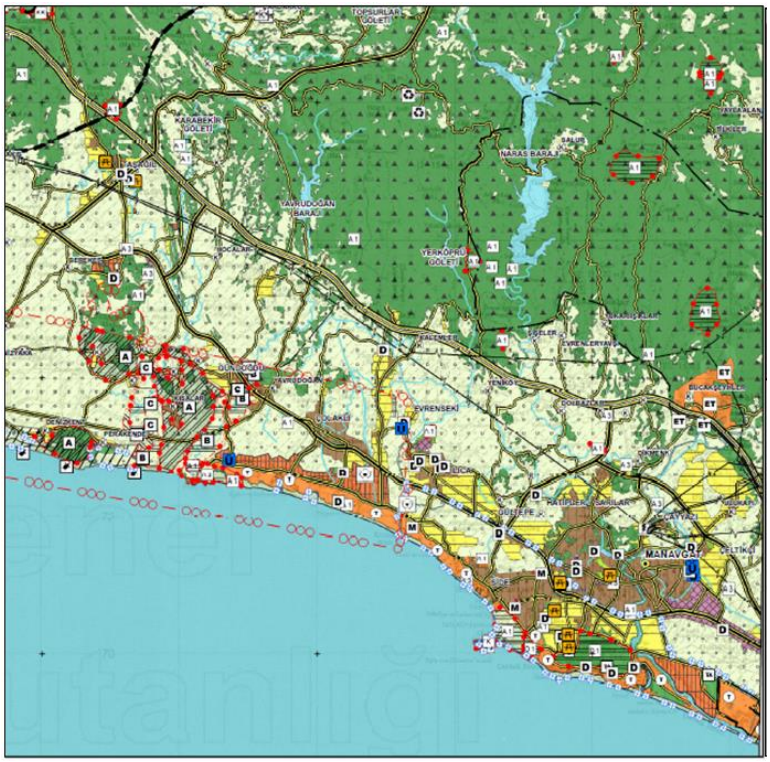

Figure 15. Manavgat environmental layout plan [47]

The 12th Development Plan, covering the period 2024-2028, Development Plan emphasises the need for pre-disaster preparedness measures in cities against disaster risks. This has shaped the objective of the 1/100,000-scale Environmental Planning Scheme for the Antalya-Burdur-Isparta Planning Region, targeting 2025, to define the region's protection and development objectives and strategies. The plan aims to achieve a balance between conservation and use, protect natural, historical and cultural values, and develop agriculture and forestry while preserving fertile agricultural land, forest areas and sensitive ecosystems. Furthermore, diversifying tourism and ensuring its sustainability are also among the plan's priorities. In this context, the environmental plan establishes a guiding framework for sub-scale physical plans that take into account disaster risks and are based on the sustainable use of natural resources and the safe development of settlements. The explanatory report of the environmental plan states that the floodplain boundaries determined by the General Directorate of State Hydraulic Works and the relevant regional directorates in the master and implementation zoning plans, and the conditions for implementation relating to these areas, will be complied with. No new development projects or building permits may be issued in areas at risk of flooding. In urban settlement areas, population growth must be monitored regularly, taking into account disaster risks; necessary measures must be taken in areas of excessive density to ensure a balanced distribution of the population [47].

Method

Due to the existence of numerous criteria affecting flood risks (slope, elevation, land use, etc.), the Analytic Hierarchy Process (AHP) method was preferred; analyses were conducted in a Geographic Information System (GIS) environment, taking into account the spatial nature of the data. The risk maps obtained were evaluated not only with geographical data but also in conjunction with planning decisions, and risk maps were assessed comparatively with physical and spatial impacts. Safe, flood-free areas have been identified. In this regard, both existing risk areas have been assessed using a disaster-focused planning approach and spatially safe areas have been proposed for new settlement areas. This methodological integration stands out as the original contribution of the study.

In the literature, floods are considered a complex natural disaster involving not only geographical and climatic factors but also changes in land use due to human activities (Table 1), [48,49].

Table 1. Criteria used in flood risk analysis

Criteria	Explanations
Land Use (AK)	Land use classes exhibit different risks and potential depending on their water permeability characteristicsIn residential and mining areas, rainwater runs off rapidly due to surface impermeability, posing a high risk of flooding. Agricultural land and dunes pose a high risk due to their saturated structures. The risk is moderate in sparsely vegetated areas and low in forest, pasture and meadow areas. Bare rock surfaces pose the lowest risk because they do not produce floods due to their surface roughness [48].
Linearity Density (ÇY)	Increased linearity raises the groundwater level and reduces the risk of flooding [2,50].
Drainage Line Density (DHY)	Excessive drainage density causes surface water to flow rapidly, increasing the risk of flooding [51].
Drainage Line (DH)	Areas close to the drainage line are at high risk of flooding [48,52].
Slope Classes (E)	The risk of flooding is high in flat areas where rainfall accumulates due to reduced slope values [53].
Lithology (L)	Impermeable rocks increase surface runoff and heighten the risk of flooding due to their low water permeability. In rocks that easily allow water to pass through, the opposite is true [54,55].
Soil Texture (T)	Impermeable soils increase flood risk, while permeable soils reduce flood risk [56,22].
Annual Rainfall Amount (Y)	As rainfall increases, the risk of flooding increases [49].
Elevation Classes (YÜ)	Surface water formed by rainfall in high-altitude areas flows to low-altitude areas, causing water to accumulate and increasing the risk of flooding [55].

The joint assessment of natural and physical variables in disaster risk analyses contributes to the modelling of disaster scenarios in a more comprehensive, consistent and realistic manner [49]. Once the criteria have been determined, the AHP is applied. Scoring (weight values) based on the scored preference scale (1-9) in Table 2 is carried out according to expert opinions or literature reviews in order to determine the relative importance of the criteria in the hierarchy with respect to other criteria [16].

Table 2. AHP importance scale [15]

Importance Scale	Definition	Explanation
1	Equally important	Both options are equally important.
3	Moderately important	Experience and judgement make one criterion slightly superior to the other.
5	Extremely important	Experience and judgement make one criterion considerably superior to the other.
7	Even more significantly important	One criterion has been deemed superior to another.
9	Definitely important	Evidence demonstrating that one criterion is superior to another is highly reliable.

2,4,6,8,	Intermediate values	Values between two consecutive judgements to be used when reconciliation is required.

The weighting of variables, their attributes, and risk scores were determined using the literature review in Table 1. According to the literature review, values between 1 and 9 (both inclusive) were assigned to the criteria to create the weights in Table 3.

Table 3. Analysis data and explanations

Criterion	Weigh t	Attributes	Risk Score	Effect	Explanation
Land Use (LU) (Class)	5	Settlemen t and Mining Areas	5	The Most	Due to impermeable surfaces in settlement and mining areas, rainwater rapidly turns into surface runoff, increasing the risk of flooding; agricultural land and dunes have been assigned a high risk score as they are saturated. Due to the reduction in surface runoff caused by vegetation cover, sparse vegetation areas, medium forests, pastures and meadows have been assigned a low risk score. Bare rock surfaces have been assigned the lowest risk score as their roughness slows down the flow.
		Agricultur al Land and Dunes	4	Very Much	
		Sparse Plant Areas	3	Centre	
		Mera, Meadow and Forest Areas	2	Less	
		Bare Rocks	1	At least	
Linear Density (LD) (Km/Km²)	3	0-0.052	5	The Most	As the increase in linearity density enhances the water's infiltration capacity into the ground, the risk of flooding decreases in areas with high density.
		0.053-0,15	4	Very Much	
		0,16-0,24	3	Centre	
		0,25-0,36	2	Less	
		0,37-0,6	1	At least	
	7	0-1.6	1	At least	

Drainage Density (DD) (Km/Km²)		1.7-3.1	2	Less	For flood risk, 5 points are assigned to the class with the highest drainage intensity value and 1 point to the class with the lowest value.
		3.2-4.5	3	Centre	
		4.6-6.4	4	Very Much	
		6.5-11	5	The Most	
Drainage Line (DL) (Metre)	7	0-100	5	The Most	Areas close to the drainage line have been given 5 points as they are at the highest risk of flooding, while distant areas have been given 1 point.
		100-200	4	Very Much	
		200-300	3	Centre	
		300-400	2	Less	
		400-500	1	At least	
Slope Classes (S) (Degree)	6	0-7,6	5	The Most	As the slope decreases, the risk of flooding increases; therefore, low-slope areas have been assigned 5 points and high-slope areas 1 point.
		7,7-16	4	Very Much	
		17-24	3	Centre	
		25-35	2	Less	
		36-81	1	At least	
Lithology (L) (Class)	5	Alluvial	5	The Most	Areas with alluvial rock formations are saturated with water, making them most at risk of flooding. Due to the low water permeability of shale, rubble and olistostrome rocks, the risk of flooding is high. The risk of flooding is moderate in conglomerate, sandstone and volcanic sedimentary rocks, as the amount of water seepage is moderate. Although marble has a low water permeability capacity, it allows water to seep into the ground due to its fractured and
		Kiltaşı, Rubble (Colluvial) and Olilostrom	4	Very Much	
		Conglomerate, Aeolian and Volcanic Sedimentary Rocks	3	Centre	
		Marble	2	Less	
		Limestone, Calcareous Limestone and Dolomite	1	At least	

					cracked structure. For this reason, a low risk score has been assigned. Limestone, marly limestone and dolomite have the lowest risk of flooding because water passes through them easily.
Soil Texture (ST) (Class)	5	Alluvial Soil	5	The Most	In alluvial soils, the groundwater level is high, so water seeps into the ground only to a limited extent. For this reason, a high risk score has been assigned. In sandy soils, water permeates the soil more effectively.
		Sandy Soil	3	Centre	
Annual Rainfall Amount (AR) (Mm)	8	530-580	1	At least	As rainfall increases the risk of flooding, 5 points were awarded to the category with the highest rainfall and 1 point to the category with the lowest rainfall.
		590-630	2	Less	
		640-680	3	Centre	
		690-730	4	Very Much	
		740-780	5	The Most	
Elevation Classes (E) (Metre)	6	18-310	5	The Most	As elevation decreases, flood risk increases; therefore, the lowest areas have been assigned 5 points, while the highest areas have been assigned 1 point.
		320-690	4	Very Much	
		700-1100	3	Centre	
		1200-1600	2	Less	
		1700-2500	1	At least	

The 9-dimensional pairwise comparison matrices presented in Table 4 were created in accordance with the weights in Table 3. The variables on the diagonal of the matrix take the value 1 because they are compared with themselves. The other components are determined according to the level of importance of the variables relative to each other. For example, when comparing the initial weight values (I.W.V) of the first variable (Land Use - LU) and the second variable (Linearity Density - LD), the first row and second column element of the matrix (LU = 5, LD = 3) will take the value (5/3) 1.67. Otherwise, it will take the value 0.60 (3/5).

Table 4. AHP decision matrix

İ.W.V	**Criterion**	**LU**	**LD**	**DD**	**DL**	**S**	**L**	**ST**	**AR**	**E**

5	LU	1,00	1,67	0,71	0,71	0,83	1,00	1,00	0,63	0,83
3	LD	0,60	1,00	0,43	0,43	0,50	0,60	0,60	0,38	0,50
7	DD	1,40	2,33	1,00	1,00	1,17	1,40	1,40	0,88	1,17
7	DL	1,40	2,33	1,00	1,00	1,17	1,40	1,40	0,88	1,17
6	S	1,20	2,00	0,86	0,86	1,00	1,20	1,20	0,75	1,00
5	L	1,00	1,67	0,71	0,71	0,83	1,00	1,00	0,63	0,83
5	ST	1,00	1,67	0,71	0,71	0,83	1,00	1,00	0,63	0,83
8	AR	1,60	2,67	1,14	1,14	1,33	1,60	1,60	1,00	1,33
6	E	1,20	2,00	0,86	0,86	1,00	1,20	1,20	0,75	1,00
Total (≈)		10,4	17,3	7,43	7,43	8,67	10,4	10,4	6,5	8,67

As shown in Table 4, after calculating the weights of the criteria in the matrix relative to each other, the sum of each column was taken separately, and the normalisation process was performed by dividing the value in each cell by the sum of that column. For example, the value 1 in the first column of the first row has been normalised to approximately 0.10 by dividing it by the sum of the first column, which is 10.40. This process was applied uniformly to all cells in the tables to create a table of normalised weight values (Table 5).

Table 5. Normalised weight values

Criterion	**LU**	**LD**	**DD**	**DL**	**S**	**L**	**ST**	**AR**	**E**	**Priority Vector (W_i)**
LU	0,10	0,10	0,10	0,10	0,10	0,10	0,10	0,10	0,10	0,10
LD	0,06	0,06	0,06	0,06	0,06	0,06	0,06	0,06	0,06	0,06
DD	0,13	0,13	0,13	0,13	0,13	0,13	0,13	0,13	0,13	0,13
DL	0,13	0,13	0,13	0,13	0,13	0,13	0,13	0,13	0,13	0,13
S	0,12	0,12	0,12	0,12	0,12	0,12	0,12	0,12	0,12	0,12
L	0,10	0,10	0,10	0,10	0,10	0,10	0,10	0,10	0,10	0,10
ST	0,10	0,10	0,10	0,10	0,10	0,10	0,10	0,10	0,10	0,10
AR	0,15	0,15	0,15	0,15	0,15	0,15	0,15	0,15	0,15	0,15
E	0,12	0,12	0,12	0,12	0,12	0,12	0,12	0,12	0,12	0,12
Total	1	1	1	1	1	1	1	1	1	1

After normalisation, the W_i value, which indicates the weight of the criterion related to the arithmetic mean of each row among the other criteria, has been determined. Following this process, the values in the comparison matrix containing each criterion were multiplied by the previously obtained criterion weights to calculate the A × W vector. The weighted sum vector (AW_i) was found by taking the sum of the products for each row (Table 6).

Table 6. Weighted Total Vector Values

Criterion	**W_i**	**AW_i**
LU	0,10	0,81
LD	0,06	0,28
DD	0,13	1,64
DL	0,13	1,64
S	0,12	1,18
L	0,10	0,81
ST	0,10	0,81
AR	0,15	2,19
E	0,12	1,18

After this step, λ_{max} its value is calculated.

$$\lambda_{max}=\sum \frac{AW_i}{W_i}=9.91 \quad (1)$$

Obtained for the consistency calculation λ_{max} by using CI (Consistency Index) calculated. CI, It is a measure that indicates the degree of consistency of the comparison matrix.

$$CI=\frac{\lambda_{max}-n}{n-1} = CI=\frac{9.91-9}{9-1}=0.11 \quad (2)$$

RI (15 kriter için):1.59 [57].

$$CR=\frac{CI}{RI}=\frac{0.11}{1.45}=0.08 \quad (3)$$

CR = 0.08< 0.10 → These calculations have resulted in consistency, and the analysis performed is valid. Thus, the weights of the criteria have been reliably determined and entered as integer values (Table 7).

Table 7. Conversion of weight values to whole numbers

Criterion	Weight Values (W_i)	Percentage (%)
LU	0,10	%10
LD	0,06	%5
DD	0,13	%13
DL	0,13	%13
S	0,12	%12
L	0,10	%10
ST	0,10	%10
AR	0,15	%15
E	0,12	%12

Flood Risk Map = (LU×0.10)+….+(Ex0.12) formülü ile oluşturulmuştur [53,57]. In this process, a flood risk map is created by calculating the weighted totals of all criterion maps. The resulting risk map is categorised to make the analysis results more understandable. These classes represent levels such as low, medium and high risk.

Results

Located approximately 4-5 kilometres inland from the coast, on relatively flat terrain, the city centre of Manavgat is surrounded by the Taurus Mountains to the north, whose elevation gradually increases, and the Mediterranean Sea to the south. Due to this topography, local variations in climate characteristics are observed as the elevation increases towards the north. Between the coast and the foothills, numerous plains of varying sizes have formed as a result of the accumulation of alluvial material carried by rivers. The Taurus Mountains, running east–west parallel to the Mediterranean Sea, have enabled Manavgat to develop northwards, and the city has expanded in all directions. Although rainfall is predicted to increase by approximately 5 per cent by 2040, it would be incorrect to attribute the flood risk in Manavgat on the Mediterranean coast solely to rainfall. This is because it is known that strong southerly winds prevent river flow from reaching the sea, and occasionally, the simultaneous effects of wind and rainfall further trigger flooding and flash floods. The proximity of historical structures to the sea increases the likelihood of not only material and moral losses but also cultural losses.

From the 1900s onwards, settlement increased in the centre of Manavgat, with urbanisation concentrated particularly in the gently sloping alluvial soils between the Taurus Mountains and the Mediterranean Sea, significantly increasing the risk of flooding. The Manavgat River, located in this region, has also been a factor increasing the risk due to its flood potential. The marshes formed by the Manavgat River in the past are also related to floods; however, with the draining of these marshes in the 1950s, settlement began to develop in the western direction of the city.

Since the 1970s, many forested areas have been destroyed in order to expand agricultural land. The construction of roads cutting across the Manavgat River between 1984 and 1990, coupled with the

acceleration of tourism activities after 1986 and increased development in forested areas, has further heightened the risk of flooding. Furthermore, the failure to prepare development plans in accordance with higher-level and prescriptive plans such as environmental plans has led to uncontrolled construction around rivers in city centres, paving the way for the formation of areas with a high risk of flooding.

In Manavgat district, flood risk varies over short distances due to the variability of geological, topographical, climatic and land use characteristics over short distances. For this reason, criterion maps have been created (Figure 16) with the aim of analysing the risk distribution.

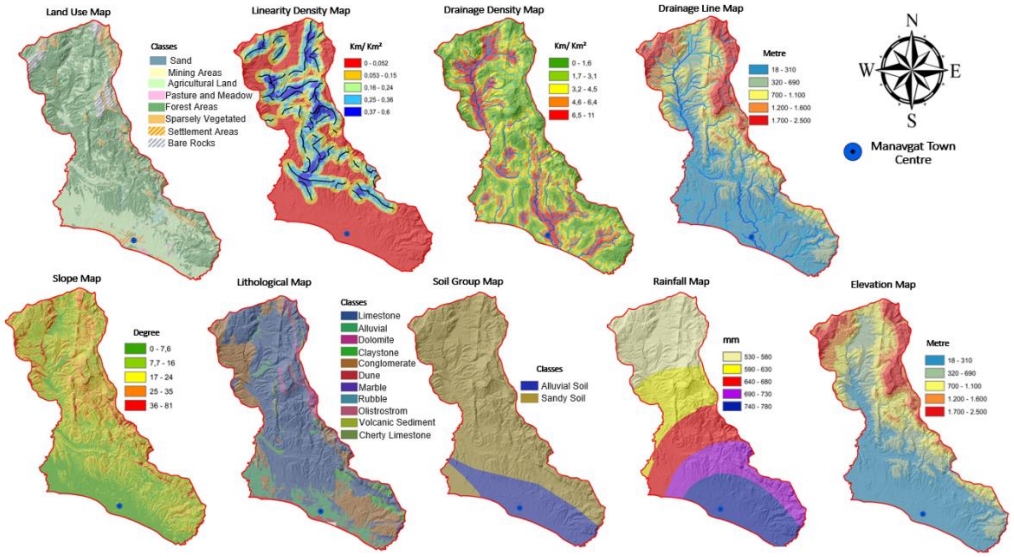

Figure 16. Criteria maps produced for flood risk

When examining the land use map prepared based on data from the Copernicus land monitoring service [58], In the northern section, forested areas, sparse vegetation areas, bare rock formations and agricultural land are prevalent; in the east, forested areas, sparse vegetation areas and bare rock formations are again prevalent; in the west, forested areas and agricultural land are widespread; while in the south, agricultural land and settlement areas predominate. The linearity density map created using a digital elevation model [59] shows that the density is high in the east, north and west, respectively, and negligible in the south. The drainage line density map based on the same model [59] shows that the density is very high in the south and north-west regions, moderate in the west, and very low in the east. The drainage line map [59] shows that areas passing through the city centre, particularly in the northeast and south, contain more drainage lines than other areas. Upon examination of the slope map [59], it was determined that the slope is high in the north, north-west and east, while it is quite low in the southern sections where the city centre is located. The elevation map prepared using the digital elevation model [59] indicates that the elevation is high in the northeast and northwest, gradually decreasing towards the south. In the lithology map prepared using mining exploration data [60] shows that limestone, conglomerate, dolomite and claystone prevail in the north; conglomerate, alluvium and limestone in the east; limestone, dolomite, conglomerate and claystone in the west; and alluvial units, conglomerate and limestone in the south. The soil group map [61], prepared according to data from the Ministry of Agriculture and Forestry, reveals that alluvial soils predominate in the south, while sandy soils are predominant in other regions. The rainfall map created using data from the General Directorate of Meteorology [62] shows that annual rainfall increases from north to south. These criteria maps alone are not sufficient for flood risk analysis. A more accurate risk analysis is performed by cross-referencing each criterion according to its impact and importance levels and preparing a risk analysis map. According to the flood risk map obtained by overlaying the criteria maps (Map 2), the class covering the largest area in the city is the high-risk class. This is followed by the medium, low, very high and very low risk classes respectively.

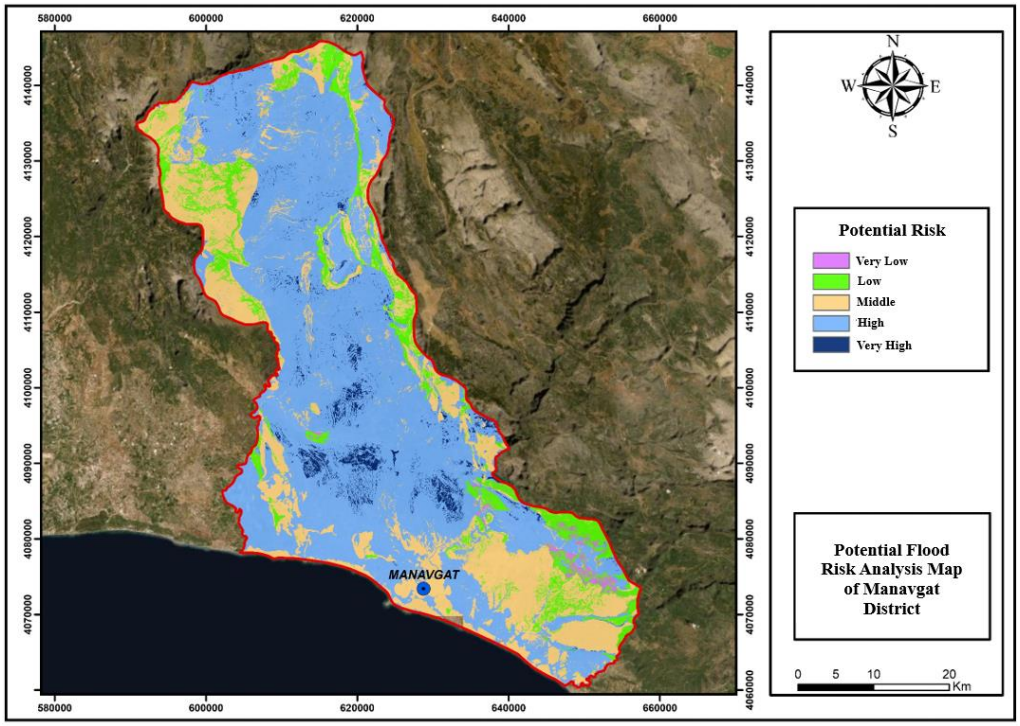

Map 2. Manavgat flood risk analysis map

According to the flood risk analysis map, areas in Manavgat with moderate to high rainfall amounts where the elevation has decreased, and areas with alluvial and sandy soil types have been identified as being at very high risk. The city centre of Manavgat has been classified as medium to high risk. Areas with forested land have mostly been found to be low risk. Very low-risk areas are generally forested areas with high elevation.

When examining the immediate vicinity of the city centre, the presence of high-risk areas in the north-west to south-east direction is noteworthy. This also confirms that it is parallel to the direction of the south-westerly winds. On the other hand, there are medium-risk areas in the east, west, north and south. Planning permission in these areas should be granted with consideration for flood risk, and the risk ratio should be reduced.

Discussion

The increasing risk of disasters in Turkey due to climate change and changes in land use has necessitated legal regulations requiring risk-focused approaches in planning processes. Numerous legal regulations have been enacted in high-level plans, but flooding continues in expanding urban areas before the legal regulations come into force.

It is evident that the risk of flooding in Manavgat stems from both natural climatic conditions and human activities. Following the 1970s, the expansion of urban areas alongside population growth and the reduction of forested areas to increase agricultural land have made the region more vulnerable to floods and landslides. The uncontrolled development of flood-prone areas has disrupted surface runoff, reduced the effectiveness of drainage systems, and made it more difficult for rainwater to infiltrate the soil due to the increase in impervious surfaces. This situation has caused water to accumulate rapidly on the surface and increased the risk of flooding.

Conclusions

The flood risk analysis map provides an important basis for strategies to reduce disaster risk in Manavgat. In the face of increasing population and development pressure, it is of great importance to protect productive agricultural land and to prepare development plans taking into account population projections and the carrying capacity of the natural environment. Furthermore, protecting existing green spaces, preventing development in marshes and wetlands, and avoiding the destruction of forested

areas to gain agricultural land will contribute to both preserving the natural balance and reducing flood risk.

As there are high-risk areas in the north-west to south-east direction in the immediate vicinity of the city centre, planning permission should be granted as little as possible, and urban development should be encouraged towards the east, west, north and south. In these medium-risk areas, planning permission should be granted in a controlled manner, taking into account the risk of flooding and landslides.

Funding Not Applicable.

Data Availability Statement No datasets were generated or analysed during the current study.

Declaration

Clinical trial number: Not applicable.

Ethics declaration: Not applicable.

Consent to Participate declaration: Not applicable.

Consent to publish: Not applicable.

Competing interests The authors declare no competing interests.

References

1. Amil, T. A. (2018). Determining of different inundated land use in Salyan Plain during 2010 the Kura River flood through GIS and remote sensing tools. International Journal of Engineering and Geosciences (IJEG), 3(3), 080–086. https://doi.org/10.26833/ijeg.412348
2. Chen, W., Li, Y., Xue, W., Shahabi, H., Li, S., Hong, H., Wang, X., Bian, H., Zhang, S., Pradhan, B., & Ahmad, B. Bin. (2020). Modeling Flood Susceptibility Using Data-Driven Approaches Of Naïve Bayes Tree, Alternating Decision Tree, And Ran-dom Forest Methods. Science of the Total Environment, 701, 134979. https://doi.org/10.1016/j.scitotenv.2019.134979
3. Utlu, M. (2023). Frekans Oranı ve Shannon Entropisi Yöntemi Kullanarak Ezine Çayı Havzası Taşkın Duyarlılık Analizi (Kastamonu-Bozkurt). Jeomorfolojik Araştırmalar Dergisi, (11), 160-178. https://doi.org/10.46453/jader.1358845
4. Ergül, T., & Aydın, O. (2025). Küçük Melen İğneler Havzası'ndaki Taşkınların Hidrolojik Modelleme Yöntemiyle (HEC-HMS) Belirlenmesi. Geomatik, 10(1), 1-14. https://doi.org/10.29128/geomatik.1492923
5. Simoes-Sousa, I. T., Camargo, C. M., Tavora, J., Piffer-Braga, A., Farrar, J. T., & Pavelsky, T. M. (2025). The May 2024 flood disaster in southern Brazil: Causes, impacts, and SWOT-based volume estimation. Geophysical Research Letters, 52(4), https://doi.org/10.1029/2024GL112442
6. Tellman, B., Sullivan, J. A., Kuhn, C., Kulp, S., Doyle, C. S., & Shepherd, T. G. (2024). Global exposure to extreme flood events under future climate and demographic change. Nature Communications, 15, 5664. Erişim Adresi: https://ui.adsabs.harvard.edu/abs/2024AGUFMH23T...04T
7. Berghuijs, W. R., Harrigan, S., Molnar, P., Slater, L. J., & Kirchner, J. W. (2019). The Relative İmportance Of Different Flood-Generating Mechanisms Across Europe. Water Resources Research, 55(6), 4582-4593. https://doi.org/10.1029/2019WR024841
8. T.C. Tarım ve Orman Bakanlığı. (2022). Taşkın Yönetimi. Erişim Adresi: https://www.kisa.link/cCFXz
9. ÇŞİDB, (2025). Çevre, Şehircilik ve İklim Değişikliği Bakanlığı Meteoroloji Genel Müdürlüğü. Meteoroloji 2024 Yılı İklim Değerlendirmesi. Erişim Adresi: https://www.mgm.gov.tr/
10. Gayen, A., & Saha, S. (2018). Deforestation Probable Area Predicted By Logistic Regression In Pathro River Basin: A Tribu-tary Of Ajay River. Spatial Information Research, 26(1), 1-9. https://doi.org/10.1007/s41324-017-0151-1
11. Deng, P., Bing, J., Wang, L., & Li, L. (2025). Extreme rainfall frequency distribution and its flood risk assessment in the Up-per Hanjiang River Basin. Natural Hazards, 1-20. https://doi.org/10.1007/s11069-025-07313-0
12. Sabancı, S. (2012). Alanya ve Manavgat'ın iklim özellikleri. (Yayımlanmamış Yüksek Lisans Tezi. İstanbul Üniversitesi Sosyal Bilimler Enstitüsü, İstanbul, Türkiye)
13. AFAD. (2021). İl Afet Risk Azaltma Planı. T.C. Antalya Valiliği İl Afet Acil Durum Müdürlüğü. Erişim Adresi: https://antalya.afad.gov.tr/kurumlar/antalya.afad/Tasarim/IRAP/Antalya-IRAP_2022.pdf
14. Manavgat Belediyesi. (2024). Haber Arşivi. Erişim Adresi: https://www.manavgat.bel.tr/guncel-haberler/manavgat-belediyesi-siddetli-yagisin-ardindan-vatandaslarin-yaninda
15. Saaty, T. L. (1980). The Analytic Hierarchy Process. Mcgraw Hill, New York. Agricultural Economics Review, 70(804), 10-21236.

16. Malczewski, J. (1999). GIS And Multicriteria Decision Analysis. John Wiley & Sons, Inc. ISBN: 978-0-471-32944-2 Erişim Adresi: https://www.kisa.link/ePpUn
17. Moghadas, M., Asadzadeh, A., Vafeidis, A., Fekete, A., & Kötter, T. (2019). A Multi-Criteria Approach For Assessing Urban Flood Resilience İn Tehran, Iran. International Journal of Disaster Risk Reduction, 35, 101069. https://doi.org/10.1016/j.ijdrr.2019.101069
18. Jagtap, A. A., Shedge, D. K., Degaonkar, V., & Chowdhary, V. R. (2023, March). Flood Risk Area Identification of Pune Dis-trict using GIS Techniques. In 2023 9th International Conference on Advanced Computing and Communication Systems (ICACCS) (Vol. 1, pp. 1326-1331). IEEE. Erişim Adresi: https://ieeexplore.ieee.org/stamp/stamp.jsp?arnumber=10112874
19. Li, S., & Mo, H. (2011). Risk Zoning Of Flood Disaster Based On GIS: A Case Study Of Xiangjiang River, Hunan Province, China. In 2011 International Conference on Remote Sensing, Environment and Transportation Engineering .2452-2455. https://doi.org/10.1109/rsete.2011.5964809
20. Ocak, F. (2023). Ladik Gölü Havzası'nda (Samsun) Akıllı Doğal Afet Yönetimi. (Doktora Tezi. Ondokuz Mayıs Üniversitesi. Lisans Üstü Eğitim Enstitüsü. Samsun, Türkiye)
21. Bingöl, F., Yıldırım, İ. H., Aytaç, AS, Kaylı, Ö., Abukan, S. ve Polat, N. (2023). A GIS-Based Study of the Causes of the Flood Disaster that Occurred in the City Centre of Şanlıurfa (Turkey) in 2023. Intercontinental Geoinformation Days , 6 , 171-175. Erişim Adresi: https://www.researchgate.net/publication/390482910
22. Değerliyurt, M. (2013). Antakya'da Doğal Afet Risk Analizi ve Yönetimi. (Doktora Tezi. İstanbul Üniversitesi. Sosyal Bilimler Enstitüsü) Erişim Adresi: https://www.kisa.link/pGhdP
23. Aksoy, H. (2024). Su Duyarlı Kentler: Manavgat Kenti Özelinde Bir Değerlendirme, (Yüksek Lisans Tezi. Ankara Üniversi-tesi. Fen Bilimleri Enstitüsü. Kentsel Tasarım Ana Bilim Dalı) Erişim Adresi: https://l24.im/DkcvzH3
24. Asker, İ. (2015) Manavgat Kentinin Özellikleri ve Kent Merkezinin Trafik Sorunu ve Çözüm Önerileri, (Yüksek Lisans Tezi. Fen Bilimleri Enstitüsü. Bahçeşehir Üniversitesi. İstanbul) Erişim Adresi: https://tez.yok.gov.tr/UlusalTezMerkezi/tezDetay.jsp?id=I_H2Z4NqiQ16nv_A9KknZw&no=ylmFOt0iKSFEEuSPZqQxlw
25. Dinç, Y. (2020). Karşılaştırmalı Bir Şehir Coğrafyası: Alanya ve Manavgat Örneği. (Doktora Tezi, Marmara Universitesi. Sosyal Bilimler Enstitüsü) Erişim Adresi: https://www.kisa.link/syGKl
26. Ak, M.M. (2019). Manavgat İlçesinin Ekonomik Coğrafyası, (Yayımlanmamış Yüksek Lisans Tezi. Ondokuz Mayıs Üniver-sitesi, Sosyal Bilimler Enstitüsü) Erişim Adresi: https://l24.im/ZewfA5
27. Yıldırım, Ş. (2013). Side Antik Kentinin Bizans Dönemi Dini Mimarisi. (Doktora Tezi, Anadolu Üniversitesi.Sosyal Bilimler Enstitüsü. Eskişehir, Türkiye)
28. Akış, A., & Kaya, B. (2018). Manavgat'ın (Antalya) Alternatif Turizm Potansiyeli. Asya Studies, 3(3), 20-27. https://doi.org/10.31455/asya.387029
29. Zainalabden, T. I. A. (2022). Çok Kriterli Karar Analizi İle Oluşturulan Orman Yangını Risk Haritalarının Gerçekleşen Or-man Yangınları İle Karşılaştırılması (Manavgat Örneği). (Yüksek Lisans Tezi, Çankırı Karatekin Üniversitesi. Çankırı, Tü-rkiye)
30. Akengin, H., & Dinç, Y. (2018). Şehirlerin Yatay Gelişimlerinde Coğrafi Faktörlerin Etkisi: Manavgat Örneği. TÜCAUM, 30, 532-550. Erişim Adresi: https://www.kisa.link/KzuPG
31. MGM, (2014). Orman ve Su İşleri Bakanlığı, Meteoroloji Genel Müdürlüğü, Araştırma Dairesi Başkanlığı Araştırma Dairesi Başkanlığı, 2014 Yili Iklim Değerlendirmesi. Erişim Adresi: https://www.mgm.gov.tr/files/iklim/2014-yili-iklim-degerlendirmesi.pdf
32. MGM, (2024). Meteoroloji Genel Müdürlüğü, İklim ve Tarımsal Meteoroloji Araştırma Dairesi Başkanlığı. Erişim Adresi: https://www.mgm.gov.tr/veridegerlendirme/il-ve-ilceler-istatistik.aspx?m=ANTALYA
33. Karaoğlu, M. (2018). Rüzgar ve Rüzgar Olayları. Journal of Agriculture, 1(2), 39-48. Erişim Adresi: https://dergipark.org.tr/en/download/article-file/612656
34. Şahin, K., & Bağcı, H. R. (2015). Türkiye'de Lodos'un Sinoptik Klimatolojisi (Samsun İli Örneği). Journal Of International Social Research, 8(40). ISSN: 1307-9581. Erişim Adresi: https://research.ebsco.com/c/mwvn5v/viewer/pdf/m4a724pafr
35. Tümer, S., Kurt, M., & Hepokur, F. (2022). Antalya'da ırmak taştı, iş yerleri ve tarım alanlarını su bastı. Haber. Antalya, Manavgat, Türkiye: Anadolu Ajansı. Erişim Adresi: https://www.aa.com.tr/tr/gundem/antalyada-irmak-tasti-is-yerleri-ve-tarim-alanlarini-su-basti/2471809
36. DSİ. (2021). (Devlet Su İşleri). 13.Bölge Müdürlüğü. Erişim Adresi: https://bolge13.dsi.gov.tr/
37. Aydınözü, D. (2004). Side'nin Turizm Potansiyeli. Gazi Eğitim Fakültesi Dergisi, Gazi Üniversitesi. Cilt: 24, 1, 81-97. Erişim Adresi: https://dergipark.org.tr/tr/download/article-file/77335
38. Karaca, B. (2009) XV. ve XVI. Yüzyıllarda Manavgat Kazası, Fakülte Kitapevi, Isparta. ISBN: 9789757135951
39. Konyalı, İ. H., & Yıldız, A. (2009). Abideleri ve kitabeleri ile Manavgat Tarihi. Medya Işıl.
40. Arıcı, F. (1985) Manavgat Doğusunda Coğrafi Araştırmalar (Beşeri ve Ekonomik Coğrafyası), (Yüksek Lisans Tezi. Ankara Üniversitesi. Sosyal Bilimler Enstitüsü. Ankara)
41. Tunçdemir, O. (1973) Manavgat: Tarih ve Turizm. Manavgat Matbaası, Manavgat.
42. Öz, A. (1974) Manavgat'ın Beşeri ve İktisadi Etüdü, İstanbul Üniversitesi Edebiyat Fakültesi Coğrafya Enstitüsü. (Bitirme Tezi, İstanbul. İstanbul, Türkiye)
43. Kasarcı, R. (1993). Türkiye'de nüfus gelişimi. Türkiye Coğrafyası Araştırma ve Uygulama Merkezi Dergisi, 5, 247-266. Erişim Adresi: https://www.kisa.link/lkgkf

44. Işık, Ş. (1999). 1997 Nüfus Tespiti ve Türkiye Nüfusu Üzerine Bazı Yeni Gözlemler. Ege Coğrafya Dergisi, 10(1).149-172. Erişim Adresi: https://dergipark.org.tr/tr/download/article-file/56822
45. Kao, W.-L. (2001) Manavgat ve Çevresinin Fiziki Coğrafyası, (Yüksek Lisans Tezi. Ankara Üniversitesi Sosyal Bilimler Enstitüsü. Ankara)
46. Alpaslan, Ö. (2009). Antalya Kıyı Bölgesi Planlama Sürecinin Kıyı Alanlarına Etkileri: Side Manavgat Örneği. TMMOB Şehir Plancıları Yayını, 46, 67-71. Erişim Adresi: https://www.kisa.link/ZcRcC
47. ÇŞİDB, (Çevre, Şehircilik ve İklim Değişikliği Bakanlığı) (2025). Çevre Düzeni Planı Açıklama Raporu. Mekansal Planlama Genel Müdürlüğü. Erişim Adresi: https://www.kisa.link/EvhrU
48. Abd El Aal, A., Kamel, M., & Al-Homidy, A. (2019). Using Remote Sensing And GIS Techniques İn Monitoring And Mitiga-tion Of Geohazards İn Najran Region, Saudi Arabia. Geotechnical and Geological Engineering, 37(5), 3673–3700. https://doi.org/10.1007/s10706-019-00861-w
49. İnce, A. F. (2023). Analitik Hiyerarşi Yöntemi (AHP) ve Coğrafi Bilgi Sistemleri (CBS) Kullanılarak Sel Risk Potansiyelinin Değerlendirilmesi: Isparta İli Uluborlu-Senirkent Havzası Örneği. (Yüksek Lisans Tezi. Burdur Mehmet Akif Ersoy Üniver-sitesi. Fen Bilimleri Enstitüsü)
50. Hancı, M. (2023). Burdur Havzası Yeraltı Suyu Potansiyel Bölgelerinin Morfometrik Analiz ve Analitik Hiyerarşi Prosesi Yöntemleriyle Önceliklendirilmesi.(Yüksek Lisans Tezi. Gazi Üniversitesi. Fen Bilimleri Enstitüsü)
51. Zhang, X., Mao, F., Gong, Z., Hannah, D. M., Cai, Y., & Wu, J. (2023). A disaster-damage-based framework for assessing urban resilience to intense rainfall-induced flooding. Urban Climate, 48, 101402. https://doi.org/10.1016/j.uclim.2022.101402
52. Pourghasemi, H.R., & Rahmati, O. (2018). Flood Susceptibility Mapping Using Machine Learning Methods: A Case Study from Iran. Water, 10(8), 1022. Erişim Adresi: https://doi.org/10.1016/j.catena.2017.11.022
53. Babazadeh, R. (2020). Kentsel Alanda Deprem Hasargörebilirliğin Analitik Hiyerarşi Süreci (AHS) Yöntemi Kullanılarak Değerlendirilmesi: Yenimahalle (Ankara-Türkiye) Örneği (Doktora Tezi. Gazi Üniversitesi. Fen Bilimleri Enstitüsü) Erişim Adresi: https://www.kisa.link/wDMbs
54. Selçuk, L., Selçuk, A. S., & Kasapoğlu, D. (2016). Coğrafi Bilgi Sistemleri (CBS) Tabanlı Çok Kriterli Karar Analizi (ÇKKA) Kullanılarak, Van İli Merkez İlçelerinin Kentsel Taşkın Duyarlılık Değerlendirmesi Van/Türkiye. Yer bilimleri Dergisi, 37(1), 1-18. https://doi.org/10.17824/yrb.00247
55. Rahmati, O., Pourghasemi, H. R., & Melesse, A. M. (2016). Application Of GIS-Based Data Driven Random Forest And Max-imum Entropy Models For Groundwater Potential Mapping: A Case Study At Mehran Region, Iran. Catena, 137, 360-372. https://doi.org/10.1016/j.catena.2015.10.010
56. Oba, İ. (2009). Türkiyede Sel Afetinden Etkilenen Yerleşmelerin Coğrafi Dağılışı Nedenleri ve Planlamaya Esas Çözüm Önerileri. (Yüksek Lisans Tezi. Ankara Üniversitesi. Fen Bilimleri Enstitüsü. Ankara, Türkiye)
57. Saaty, T. L., & Kearns, K. P. (1985). Analytical Planning: The Organization Of Systems. International series in modern ap-plied mathematics and computer science (1st ed.). Oxford; New York: Pergamon Press. Erişim Adresi: https://www.kisa.link/WHttW
58. Land Monitoring Service. Available online: https://land.copernicus.eu/en/products/corine-land-cover (accessed on 10.10.2025).
59. Earth Explorer. Available online: https://earthexplorer.usgs.gov (accessed on 11.10.2025).
60. Earth Data. Available online: https://search.asf.alaska.edu/ (accessed on 12.10.2025).
61. T.C. Tarım ve Orman Bakanlığı. Available online: https://www.kisa.link/dgWuI (accessed on 19.10.2025).
62. Weatherspark. Available online: https://www.kisa.link/WrxuG (accessed on 25.10.2025).